Available online at **www.joac.info**

ISSN: 2278-1862

Journal of Applicable Chemistry

2019, 8 (3):1308- 1315

(International Peer Reviewed Journal)

Application of Sucrose Density Gradient Centrifugation for Segregation of Bio-fabricated Gold Nanoparticles using *M. longifolia* Bark Extract

AnamAfaq, Saakshi Gaur, Mukti Sharma, Saurabh Yadav, Shalini Srivastava and M. M. Srivastava*

Department of Chemistry, Faculty of Science, Dayalbagh Educational Institute, Dayalbagh, Agra-282005, **INDIA**

Email: dei.smohanm@gmail.com

Accepted on 11th April, 2019

ABSTRACT

Separation and concomitant segregation of nanoparticles is one of the thrust areas of research pertaining to the application of nanoscience. Significant research efforts have been directed towards alteration in synthesis and post synthesis for the segregation of poly dispersed nanoparticles resulting specially from plant mediated green bio-fabrication of nanoparticles. Therefore, it becomes important to segregate the nanoparticles from polydispersity to homogeneity for special academic interest and various industrial applications. The present piece of work demonstrates the size and shape segregation of poly dispersed plant mediated gold nanoparticles prepared from bark extract of M. longifolia using sucrose density gradient centrifugation, as a simple, rapid and cost-effective method. Bio-fabrication of gold nanoparticles exploiting the synergistic redox potential of the secondary metabolites of bark extracts of the plant M. longifolia in a single one pot green synthesis. Bio-fabricated gold nanoparticles embedded with plant's secondary metabolites were characterized for optical properties, morphology, diffraction patterns and size. Polydispersed nanoparticles of different size (range 23-700 nm, Z-average 141 nm) were segregated using sucrose density gradient centrifugation method having zeta size (range 6-50 nm, Z-average 22 nm). The present piece of work highlights the role of sucrose density gradient centrifugation method for segregation of poly dispersed plant mediated gold nanoparticles in a simple, fast, robust and cost-effective manner.

Graphical Abstract

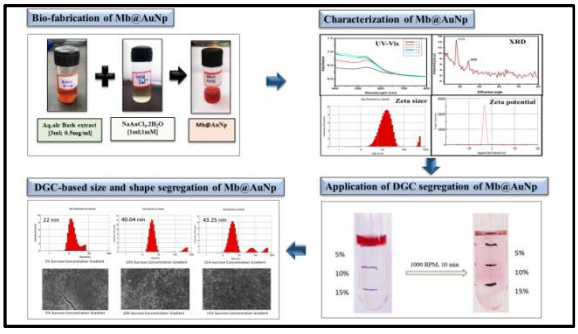

Keywords: Density Gradient Centrifugation, Plant mediated gold nanoparticles, *M. longifolia* bark extract.

INTRODUCTION

Nanoparticles possess unique physico-chemical characteristics that differ from the properties of bulk materials and strongly depend on their size and shape as a result of the quantum confinement effect [**1-6**]. Noble metals like gold and silver nanoparticles of lower size offer the best performance particularly for nano medicines and nano biotechnology. Identical nanoparticles are those having same chemical composition and dimensions. Nanoparticles having same chemical composition but different dimensions usually present different properties [**7**]. Therefore, it becomes important to know the homogeneity of the nanostructured materials for academic interest and various industrial applications. Various methods for segregation include chromatography [**8**], magnetic separation [**9**], capillary electrophoresis [**10**], selective precipitation [**11**], membrane filtration [**12**], ion pair extractions [**13**] and field flow fractionation [**14**]. Centrifugation is widely used and convenient method for nanoparticle size-based separation in solution-phase [**15, 16**]. Among the two centrifugation-based methods, density gradient centrifugation is considered better then sedimentation-based centrifugation [**17**]. Significant research efforts have been directed towards alteration in synthesis and post synthesis segregation of polydispersed nanoparticles into monodispersed homogeneous phase [**18, 19**].

The present piece of work demonstrates the segregation of gold nanoparticles using density gradient centrifugation with special reference to the effect of centrifugation speed, time and variation of shape, size and zeta potential of nanoparticles. The gold nanoparticles have been prepared using bark extract of *M. Longifolia* (Mb@AuNp) in a single pot green synthesis.

MATERIALS AND METHODS

The bark of *M. longifolia* was cleaned, shade dried and grounded into powder form. Microwave-assisted extraction of the bark was carried out in aq. alc. solution at 200W for 5 min. The extract was centrifuged (400 rpm; 10 min). The supernatant was subjected to rota-vapor distillation and finally dried by purging nitrogen. The bio-fabrication of Mb@AuNp was carried out at different pH, varied concentration of $NaAuCl_4.2H_2O$ solution, keeping bark extract constant.

Characterization of Mb@AuNp: The Mb@AuNp were characterized for optical properties using UV-Vis spectrophotometer, (Lab India, India). The morphology of Mb@AuNp was studied using FE-SEM (Nova Nano FE-SEM 450, Netherland). The X-ray diffraction pattern of Mb@AuNp was recorded using XRD (Bruker AXS D8 Advance, Germany) over 30°-80° with scan run 40 min^{-1}, step size of 0.02° and Cu Kα radiation of λ= 1.54Å. The hydrodynamic size distribution with poly-dispersity index (PDI) was analyzed using zeta sizer (Nano ZS90 model Malvern, Germany).

Density Gradient Centrifugation (DGC): Sucrose density gradient method was successfully used to fractionate anisotropic Mb@AuNp having different sedimentation rates. A discontinuous density gradient of sucrose solutions (5%, 10%, 15%) was developed upon one another. Colloidal solution of Mb@AuNp (5 mL) was added to the capacity vial and centrifuged at 1000 rpm for 30 min. Nanoparticles depending upon the size were confined to different layers. Each layer was monitored for the determination of size of particles using zeta sizer. Sedimentation coefficient S was calculated for each layer using equation:

$$S = (\rho_p - \rho_m)d^2 / 18\eta .$$

RESULTS AND DISCUSSION

Optimized experimental conditions of bio-fabricated gold nanoparticles were as follows: bark extract (3 mL, 0.5 mg mL^{-1}), sodium tetrachloroaurate dehydrate solution (1 mL, 1 mM) and sonication (15

min, 20 KHz) at pH 4. *M. longifolia* bark extract has been reported to contain polyphenolic flavonoidal compounds [20]. The conversion of Au(III) to its elemental form (Au^o) may be ascribed to the presence of flavonoidal moieties present in bark extract [21]. The visual change in color from pale yellow to ruby red indicated the bio-fabrication of target nanoparticles.

$$AuCl_4^- + 3R\text{-}OH \longrightarrow Au^0 + 3\,R{=}O + 3H^+ + 4Cl^-$$

Ultraviolet-Visible spectrophotometer: Different combinations of bark extract and $NaAuCl_4.2H_2O$ solution were analyzed by UV-VIS spectrophotometer (Figure 1). The absorption spectrums of synthesized Mb@AuNp were found to have maximum absorption band in the range of 532-540 nm. However, it was found that 1:3 ratio of bark extract and $NaAuCl_4.2H_2O$ solution had a maximum absorption band at 532 nm and further dilution doesn't show any marked increase in the absorbance. Therefore, absorption band at 1:3 ratio was considered optimum.

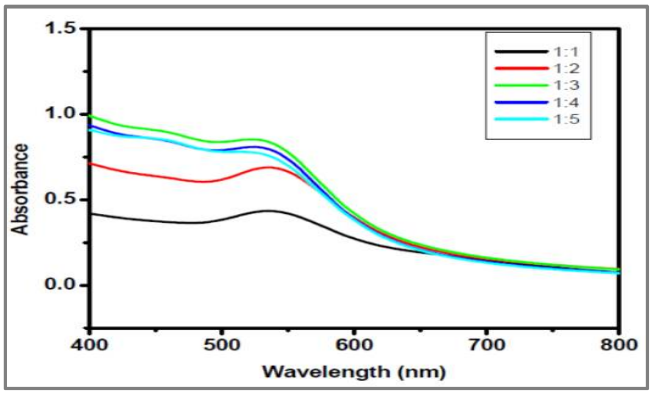

Figure 1. UV-Vis spectra of Mb@AuNp at different ratio.

X-Ray diffraction: Bragg diffraction peaks 2θ appeared at 38.4° and 44.5° in the bio-fabricated Mb@AuNp (Figure 2). It could be indexed to (111) and (200) having lattice planes of face-center cubic compared with (JCPDS file 04-0784). The intensity of the diffraction peak (200) was found lower than corresponding crystallographic plane (111). The fact established that lattice plane (111) is the transcendent crystallographic plane and is more reactive because of its high atom density [22]. The observed noise and broadening of the peak in XRD record of Mb@AuNp may be assigned to the existence of medicinally important secondary metabolites (flavonoids) loaded on the surface of bio fabricated Mb@AuNp.

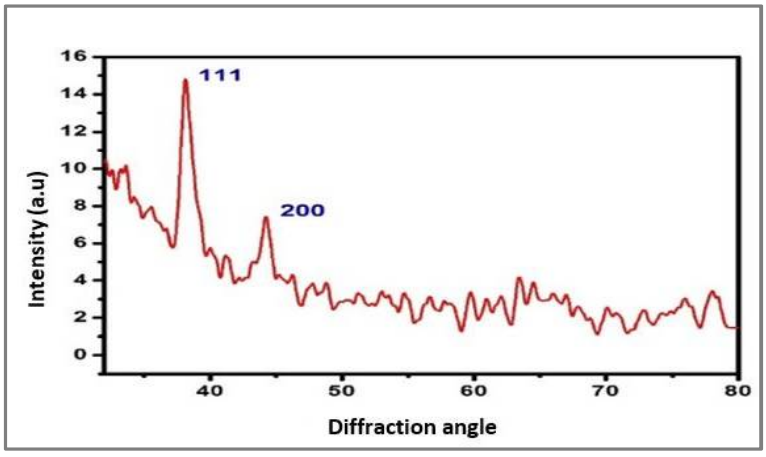

Figure 2. XRD graph of Mb@AuNp.

Dynamic light scattering: The dynamic light scattering (DLS) spectrum highlighted asymmetric distribution of nanoparticles mainly in the range (23 to 700 nm) with poly-dispersive index 0.238 **(**Figure 3a). However, a little population was extended in the range of 1500 nm. The average hydrodynamic size (Z-Average) of Mb@AuNp was found 141 nm. Zeta potential of Mb@AuNp determined in water medium as a dispersant was -31.7 mV (Figure 3b). The magnitude of observed high negative charge on the bio-fabricated nanoparticles might be acting as a repulsive barrier, avoiding aggregation of nanoparticles.

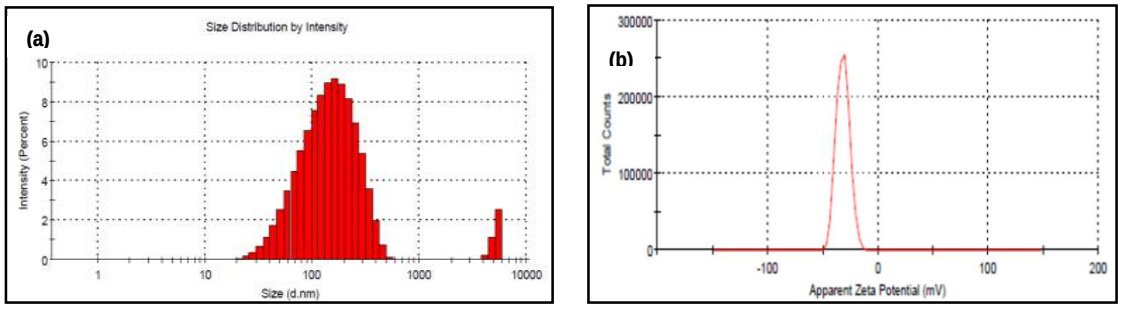

Figure 3. (a) Zeta size and (b) Zeta potential graph of synthesized Mb@AuNp.

Density Gradient Centrifugation (DGC): The size fractionation of Mb@AuNp centrifuged at 1000 rpm for fixed time(10 min) are shown in (Figure 4). Different bands obtained after the run indicated successful segregation of Mb@AuNp as per their sedimentation rates.

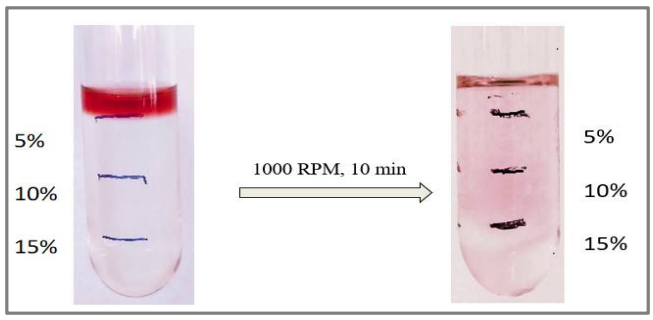

Figure 4. Optical images showing the sucrose density gradient separation of anisotropic Mb@AuNp.Images of the as-prepared parent gold nanoparticle mixture (left) and the color images (right)of the individual fractions upon successful size fractionation.

Histograms of Mb@AuNp at different sucrose concentration gradient are shown in figures 5a, b, c. It represents the distribution of the nanoparticles confined at 5%, 10%, and 15% sucrose concentration gradient. At 5% sucrose concentration gradient (Figure 5a), the distribution of nanoparticles was in the range of 06-50 nm with Z-average 22 nm. The majority of the particles lied between 10-15 nm.

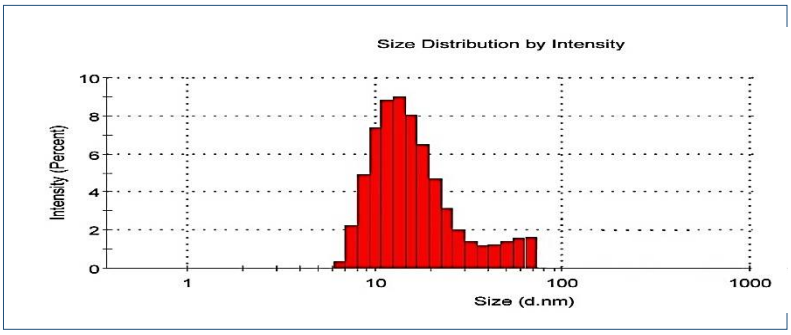

Figure 5a. Zeta size graph of 5% sucrose concentration gradient.

At 10% sucrose concentration gradient (Figure 5b), the distribution of nanoparticles was in the range of 18-100 nm with Z-average 40.04 nm. The majority of the particles lied between 30-50 nm.

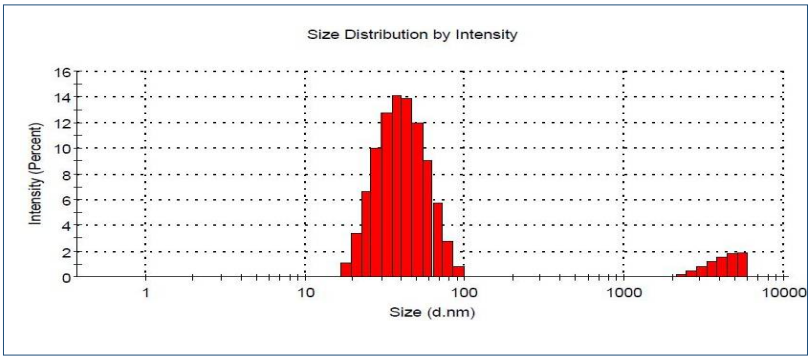

Figure 5b. Zeta size graph of 10% sucrose concentration gradient.

At 15% sucrose concentration gradient (Figure 5c), the distribution of nanoparticles was in the range of 12-110 nm with Z-average 43.25 nm. The majority of the particles lied between 30-45 nm.

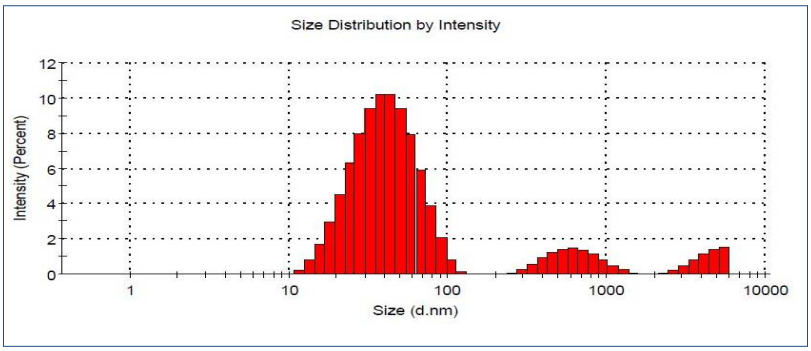

Figure 5c. Zeta size graph of 15% sucrose concentration gradient.

The above results indicate that particle size increased in a concentration-dependent manner with smaller particles occurring at lower sucrose density gradient (5%) while larger at higher density gradient (15%). This reflects that the decrease in the size of the particle takes place with a dilution of sucrose concentration gradient.

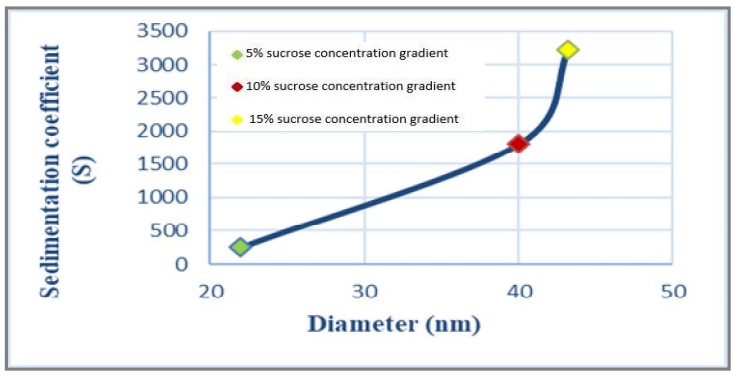

Figure 6. Variation in Sedimentation coefficient with diameter of Mb@AuNp.

Sedimentation coefficients for Mb@AuNp at 5%, 10% and 15% sucrose concentration gradient (Figure 6) were 262×10^{-3} sec, 1805×10^{-3} sec and 3225×10^{-3} sec respectively indicating faster sedimentation rate of heavier particles. Overall results obtained demonstrate the utility of density

gradient techniques to separate mixtures of different size distributions of nanoparticles to near monodispersity.

FE-SEM: FE-SEM images of Mb@AuNp (Figure 7) acquired from drop-coated films of nanoparticles indicated a change from spherical to rectangular shape via poly-dispersed morphology of Mb@AuNp bio-fabricated in the range of 5%, 10% and 15% sucrose concentration.

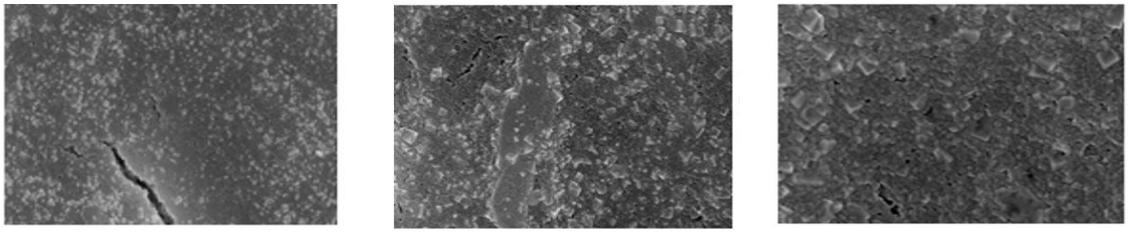

Figure 7. SEM images nanoparticles of sucrose concentration gradient 5% (left), 10%(middle) and 15% (right).

APPLICATION

The current observations signify the application of a simple, fast centrifugation method for the separation of poly-dispersed nanoparticles into monodispersed size and shape wise segregated nanoparticles providing an impetus for the study of separation techniques for the post synthesis methodologies.

CONCLUSION

A simple one-pot green synthesis of Mb@AuNp using the redox potential of the secondary metabolites of the bark extract of the plant *M. longifolia* was conducted. The density gradient centrifugation method was successfully applied to separate synthesized bio-fabricated Mb@AuNp using sucrose concentration gradient (5%, 10% and 15%).The zeta size analyses revealed that the particle size increased in a concentration-dependent manner with smaller particles occurring at lower density gradients and larger particles at higher density gradients of sucrose. Z-average size of separated Mb@AuNp confined at 5%, 10% and 15% to be 22, 40.04 and 43.25 nm. Sedimentation coefficient of larger particles was higher (3225×10^{-3} sec) compared to smaller particles (262×10^{-3} sec) indicating faster sedimentation rate of heavier particles.

ACKNOWLEDGEMENTS

The authors gratefully acknowledge Prof. P. K. Kalra, Director, Dayalbagh Educational Institute and Prof. SahabDass, Head, Department of Chemistry, Dayalbagh Educational Institute, Dayalbagh, Agra for providing necessary facilities and motivation to carry out the research.

REFERENCES

[1]. S. Balta, A. Sotto, P. Luis, L. Benea, B. Van der Bruggen, J. Kim, A new outlook on membrane enhancement with nanoparticles: The alternative of ZnO, *J. Membr. Sci.*, **2012**, 389, 155–161. DOI:10.1016/j.memsci.2011.10.025

[2]. P. Kouvaris, A. Delimitis, V. Zaspalis, D. Papadopoulos, S. Tsipas, N. Michailidis, Green synthesis and characterization of silver nanoparticles produced using Arbutus Unedo leaf extract, *Mater. Lett.*, **2012**, 76, 18-20. DOI: http://dx.doi.org/10.1016/j.matlet.2012.02.025

[3]. K. Shameli, M. B. Ahmad, E. A. Jaffar Al-Mulla, N.A. Ibrahim, P. Shabanzadeh, A. Rustaiyan, Y. Abdollahi, S. Bagheri, S. Abdolmohammadi, M.S. Usman, M. Zidan, Green

Biosynthesis of Silver Nanoparticles Using Callicarpa maingayi Stem Bark Extraction, *Molecules*, **2012**, 17, 7, 8506-8517.

[4]. S. B. Maddinedi, B. K. Mandal, S. Ranjan, N. Dasgupta, Diastase assisted green synthesis of size-controllable gold nanoparticle, *RSC Adv.*, **2015**, 5, 34, 26727–26733.

[5]. A. A. Ezhilarasi, J. J. Vijaya, K. Kaviyarasu, M. Maaza, A. Ayeshamariam, L. J. Kennedy, Green synthesis of NiO nanoparticles using Moringa oleifera extract and their biomedical applications: Cytotoxicity effect of nanoparticles against HT-29 cancer cells, *J. Photochem. Photobiol. B: Biology*, **2016**, 164, 352–360. DOI:10.1016/j.jphotobiol.2016.10.003

[6]. L. A. Dykman, N. G. Khlebtsov, Immunological properties of gold nanoparticles, *Chem. Sci*., **2017**, 8, 3, 1719–1735.

[7]. Y. Zheng, G. Feng, T. Shang, W. Wu, J. Huang, D. Sun, Y. Wang, Q. Li, Separation of biosynthesized gold nanoparticles by density gradient centrifugation, *Sep. Sci. Technol*., **2017**, 52, 5, 951–957.

[8]. C. A. Sötebier, S. M. Weidner, N. Jakubowski, U. Panne, J. Bettmer, Separation and quantification of silver nanoparticles and silver ions using reversed phase high performance liquid chromatography coupled to inductively coupled plasma mass spectrometry in combination with isotope dilution analysis, *J. Chromatogr. A.*, **2016**, 1468, 102–108. DOI:10.1016/j.chroma.2016.09.028

[9]. R. L. Oliveira, P.K. Kiyohara, L.M. Rossi, High performance magnetic separation of gold nanoparticles for catalytic oxidation of alcohols, *Green Chem.*, **2010**, 12, 1, 144–149.

[10]. M. Bouri, R. Salghi, M. Algarra, M. Zougagh, A. Ríos, A novel approach to size separation of gold nanoparticles by capillary electrophoresis–evaporative light scattering detection, *RSC Adv.*, **2015**, 5, 22, 16672–16677.

[11]. Z. Guo, X. Fan, L. Xu, X. Lu, C. Gu, Z. Bian, N. Gu, J. Zhang, D. Yang, Shape separation of colloidal gold nanoparticles through salt-triggered selective precipitation, *Chem. Comm.*, **2011**, 47, 14, 4180.

[12]. A. Akthakul, A. I. Hochbaum, F. Stellacci, A. M. Mayes, Size Fractionation of Metal Nanoparticles by Membrane Filtration, *Adv. Mater*., **2005**, 17, 5, 532–535.

[13]. C. W. Shen, T. Yu, Size-fractionation of silver nanoparticles using ion-pair extraction in a counter-current chromatograph, *J. Chromatogr. A.*, **2009**, 1216, 32, 5962–5967.

[14]. K. L. Plathe, F. von der Kammer, M. Hassellöv, J.N. Moore, M. Murayama, T. Hofmann, M.F. Hochella, The role of nanominerals and mineral nanoparticles in the transport of toxic trace metals: Field-flow fractionation and analytical TEM analyses after nanoparticle isolation and density separation, *Geochim. Cosmochim. Acta*., **2013**, 102, 213–225. DOI:10.1016/j. gca.2012.10.029.

[15]. V. Sharma, K. Park, M. Srinivasa Rao, Shape separation of gold nano rods using centrifugation, *Proc. Natl. Acad. Sci*., **2009**, 106, 13, 4981-4985.

[16]. X. Liu, J. Kang, B. Liu, J. Yang, Separation of gold nanowires and nanoparticles through a facile process of centrifugation, *Sep. Purif. Technol*., **2018**, 192, 1-4. DOI: 10.1016/j. seppur.2017.09.064.

[17]. S. H. Lee, B. K. Salunke, B. S. Kim, Sucrose density gradient centrifugation separation of gold and silver nanoparticles synthesized using Magnolia Kobus leaf extract, *Biotechnol. Bioprocess. Eng*., **2017**, 19, 1, 169-174.

[18]. Y. G. Sun, Y. N. Xia, Shape controlled synthesis of gold and silver nanoparticles, *Science*, **2002**, 298, 5601, 2176-2179.

[19]. X. Wang, Y. D. Li, Monodisperse nanocrystals: General synthesis, assembly, and their applications, *Chem. Comm.*, **2007**, 28, 2901-2910. DOI: 10.1039/b700183e.

[20]. S. Yadav, M. Sharma, N. Ganesh, S. Srivastava, M. M. Srivastava, Bioactive principle loaded gold nanoparticles as potent anti-melanoma agent: green synthesis, characterization, and in vitro bioefficacy, *Asian J. Green Chem.*, DOI: 10.22034/AJGC.2019.150792.1107.

[21]. S. Yadav, M. Sharma, N. Ganesh, S. Srivastava, M. M. Srivastava, Enhanced Anti-melanoma Bioefficacy of Flavonoid Loaded Gold Nanoparticles Prepared from the Plant Madhuca longifolia on the Mice and Human Melanoma cell lines, *J. Applicable Chem.*, **2019**, 8(2), 833-843.

[22]. G. Zhang, M. Du, X.Li, J. Huang, X. Jiang, D. Sun, Green Synthesis of Au–Ag Alloy Nanoparticles Using *Cacumen platycladi* Extract. *RSC Adv.*, **2013**, 3, 6, 1878-1884.